Influence of Ablation on the Dynamics of Slender Re-Entry Configurations

JAMES H. GRIMES JR.*
Avco Corporation, Wilmington, Mass.

AND

JOHN J. CASEY†
FluiDyne Engineering Corporation, Minneapolis, Minn.

Nomenclature

A	= reference area
C_m	= pitching moment coefficient
C_{m_α}	= $\partial C_m/\partial\alpha$
C_{m_q}	= $\partial C_m/[\partial(\dot\theta D_B/2V_\infty)]$, where $\dot\theta$ = angular velocity
$C_{m_{\dot\alpha}}$	= $\partial C_m/[\partial(\dot\alpha D_B/2V_\infty)]$
D	= reference diameter
n	= cycles
H_s/RT_0	= nondimensional enthalpy
I_{yy}	= transverse moment of inertia
$\dot m$	= ablation rate
$\dot m/\rho_\infty V_\infty A_B$	= blowing simulation parameter
$M_{\dot\theta}$	= damping moment
q^*	= heat of ablation
q	= dynamic pressure
ρ	= density
V	= velocity
α	= angle of attack
θ	= angular half amplitude
ω	= angular frequency
R	= radius
T	= temperature
Re/l	= Reynolds number/in.

Subscripts

N	= nose
B	= base
∞	= freestream
S	= stagnation
0	= supply

Introduction

THE motion of slender vehicles during entry into a planetary atmosphere is oscillatory in nature unless positive means are employed to supply stabilization (some form of attitude control such as control surfaces or jets). Vehicles that are passive in their method of stabilization would be expected to oscillate during entry. Typically, the decay in the amplitude of oscillation of a vehicle descending into the atmosphere will be governed by two factors: the effective increase in the aerodynamic "stiffness" (ρC_{m_α}) due to the increase in density during descent, and the aerodynamic damping of the vehicle, which, for a slender configuration, is proportional to

$$\exp\{\rho[-C_{L\alpha} + (C_{m_q} + C_{m_{\dot\alpha}})/(\sigma/l)^2]\}$$

During the initial, low-density phase of re-entry, the contribution of the damping term is eventually negligible. Nearly all of the damping is due to the stiffness. During late re-entry ($h \leq 200{,}000$ ft) the damping starts to be effective and becomes increasingly dominant.

Historically, predictions of the damping coefficients $C_{m_q} + C_{m_{\dot\alpha}}$ for slender bodies have been poor. Newtonian theory yields values of $C_{m_q} = -4$, and supporting ground tests (e.g., hypersonic ballistic range and free or forced oscillation wind-tunnel techniques) have yielded values of the same order, generally ranging between -4 and -10. Hypersonic flight data have yielded entirely different results, of order -100, except for a limited region of flight near the altitude of transition from laminar to turbulent flow, where positive (undamping) values have been observed. The idea that this large discrepancy between prediction and flight possibly may be due to failure to account for the effect of ablation stems from the work done originally by Syvertson and McDevitt.[1] They showed that the forced injection of gas into the air stream from the porous surface of a wind-tunnel model produced significant alteration in the level of static stability. The present note extends to the vehicle dynamics, employing a free-oscillation test technique. A direct approach to the problem has been adopted in that a "real" ablative model is employed. This choice was mainly influenced by the following considerations: 1) the use of an oscillating model minimizes the tendency toward creeping asymmetry that would otherwise be induced in a static test; and 2) an ideal test material was found in paradichlorobenzene, a low-temperature ablator, which is readily available, nontoxic, and easily handled and applied.

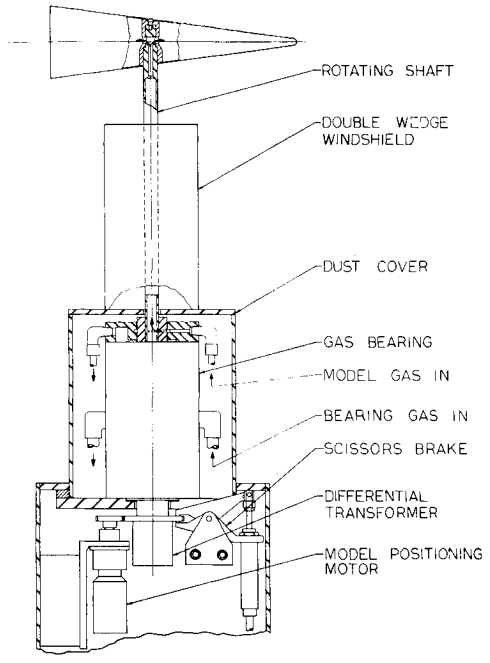

Fig. 1 High-amplitude, free-oscillation dynamic stability balance.

Equipment and Instrumentation

The dynamic stability tests were performed in the FluiDyne hypersonic blowdown wind tunnel at Mach 13.9. This is a 20-in. free jet tunnel with a Mach number uniformity of $\pm 1\%$ over a 9-in. core. The stagnation pressure and temperature for these tests were maintained at 1200 psi and 2500°R, and Re/l was 25,400/in. Most of the runs lasted 45 sec.

Dynamic stability was measured by the free oscillation method. The model was mounted on a $\frac{1}{2}$-in. hollow vertical strut that, in turn, was attached to the rotor of an air bearing, thus the model oscillated in a horizontal plane. The strut was partly protected from the air stream by a wedge airfoil wind shield (30° total angle), which extended to within 3 in. of the model centerline (Fig. 1). The $\frac{1}{2}$-in. strut diameter was selected on the basis of studies conducted at Arnold Engineering Development Center, which showed that for strut-diameter to slender-body-diameter ratios below 0.3

Presented at the AIAA Aerodynamic Testing Conference, Washington, D. C., March 9–10, 1964, under the title "Dynamic Stability Testing with Ablation at Mach 14 in a Long Duration Wind Tunnel" (no preprint number; published in bound volume of preprints of the meeting); revision received June 1, 1964.

* Group Leader, Research and Advanced Development Division, Aero-Thermo Department. Member AIAA.

† Project Engineer, Project Planning Group. Member AIAA.

there were no interference effects. This limit was not exceeded for these tests. Angular position of the model was measured with a Schaevitz RVDT with the core attached to the bearing rotor and the coil attached to the bearing stator. Waveform output was recorded on a time-based oscillograph. The passageway through the hollow strut was used to introduce secondary gas via a porous gland (essentially another air bearing) to the model used in the blowing test. Bench tests made to evaluate bearing tare damping showed that the bearing could support a moment corresponding to a 6-lb radial running load applied at the model attachment point. To assure that this load level was not exceeded, the stagnation pressure was limited to 1200 psi.

The models were either solid-wall, porous-wall, or ablating types. The solid-wall models were 0.045-in.-thick aluminum skin or 0.005-in. nickel shell. The porous-wall model (porous material over the spherical nose and a portion of the conical forebody, approximately 20% of the over-all length) employed a solid 0.005-in. nickel shell afterbody. The porous material was a sintered nickel product of 65% density. Porosity of the material is relatively uniform; hence flow distribution of the ejected gaseous nitrogen was controlled by varying the wall thickness. The ablating models were solid shells of either aluminum or nickel coated with an ablating material, ammonium chloride or paradichlorobenzene. These materials were chosen primarily for their ablative properties at relatively low temperatures and their ease of application. Since these materials are basically sublimers, the models acquired a distinct flat spot on the nose when held cocked at the initial angular displacement prior to release. This flat spot quickly disappeared from the stagnation area, however, after model release and a few cycles of oscillation. The ablation model obviously ejects gaseous products at a rate proportional to local heating; thus blowing rates are higher on the windward side. The ejection of mass via ablation could conceivably alter the boundary-layer profile; hence a phase angle relationship may exist between model and angular motion and blowing effects as the heat flux is cycled over the oscillating ablative body. Another way to express the same thought is that ablative materials may exhibit individual response times (time constants of 0.03 to 0.04 sec have been determined as meaningful in explaining flight test data). There is no doubt that a complex effect is generated by this technique. Extensive tests with many other materials at several enthalpy levels are indicated before one should adopt this relatively new test technique as infallible.

The wind-tunnel tests give the total damping moment parameter, that is, the sum of the aerodynamic and bearing damping. Total averaged damping was calculated over selected cycles from

$$M_{\dot{\theta}\text{total}} = -I_{\text{total}}/(\omega/\pi)(\ln\theta_1/\theta/n)$$

then

$$M_{\dot{\theta}\text{aero}} = M_{\dot{\theta}\text{total}} - M_{\dot{\theta}brg}$$

with $M_{\dot{\theta}brg}$ defined as a function of frequency and amplitude by bench tests prior to and immediately after the tunnel tests. The damping derivatives are obtained from

$$C_{m_q} + C_{m_{\dot{\alpha}}} = (2V_\infty/q_\infty A_B D_B^2)\cdot M_{\dot{\theta}\text{aero}}$$

The primary source of error in the damping derivative is the uncertainty in the bearing damping and the time-dependent transverse moment of inertia during the run. Generally, C_{m_α} as determined from the dynamic stability tests proved to be relatively constant over large amplitudes. This was not the case with $M_{\dot{\theta}}$ (i.e., $C_{m_q} + C_{m_{\dot{\alpha}}}$), for which considerable variations were noted. However, tests with uncoated models showed much more constant values of $M_{\dot{\theta}}$. It appeared, therefore, that most of the variation in $M_{\dot{\theta}}$ was due to an ablation rate that varied during the run. Assuming, however, that the ablation rate did not vary significantly during the relatively small number of cycles necessary for a single data point, the foregoing reduction technique is considered reasonably valid. It should be noted that the data have been adjusted for the variation in moment of inertia during a run due to ablation assuming a linear change of I_{yy} with time.

Discussion of Data Results

The data for slender-cone and cone-cylinder-flare configurations are presented in Fig. 2 with reference moment center at 61% of the unblunted length in both cases. The center of gravity indicated is a nominal value, since the mass centroid obviously changes a small amount during the run; however, translation of the center of gravity during the runs was determined to be approximately $1\frac{1}{2}$ to 3% of the model length. No coupling between pitching and heaving modes was noted because of the high shaft rigidity and also because the plane of oscillation was orthogonal to the gravity vector. Naturally, the wind-tunnel results present only laminar conditions.

Figure 2 shows the profound effect of covering a model with ablative material. Both the ammonium chloride (NH_4Cl) and paradichlorobenzene ($C_6H_4Cl_2$) ablative materials indicate similar trends in the damping parameter. Inasmuch as the $C_6H_4Cl_2$ material has a q^* of 92 Btu/lb, whereas the NH_4Cl has a q^* of approximately 1750 Btu/lb at these H_s/RT_0 levels of 18, the effect on the damping parameter of ablating $C_6H_4Cl_2$ is far more pronounced. The uncoated models with 14% bluntness ratio exhibit stable $C_{m_q} + C_{m_{\dot{\alpha}}}$ values of -4 to -5/rad. Coating the entire model with $C_6H_4Cl_2$ increased the damping by an order of magnitude to levels of -30 to -35. It is interesting to note the effect nose bluntness ratio R_N/R_B has on the dynamic stability parameter for small changes in bluntness ratio in the low bluntness ratio ranges. A 10% increase in bluntness

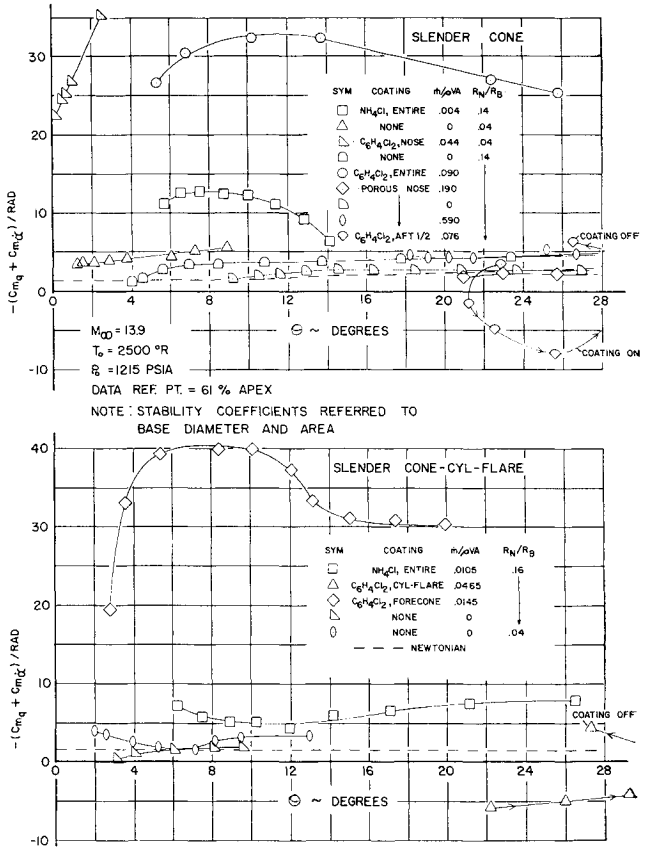

Fig. 2 Effect of mass addition to the boundary layer and bluntness ratio on the damping derivatives for slender reentry configurations.

ratio lowers C_{m_q} values by about a factor of 2 for the unablative or solid wall model tests. These same no blowing runs indicated (C_{m_α} data not presented) that the effect of increased nose bluntness ratio is to translate the aerodynamic center aft about 0.10 diam.

It was assumed as a result of preliminary examination of the data that the primary reason for increased dynamic stability with mass addition to the boundary layer was an effective shape change. It was hypothesized that coating the aft portion of the model should add an effective "flare" to the cone and possibly increase both static and dynamic stability. Runs were made with only the aft portion of the cone coated. As the data demonstrate, when the model was released, it damped slightly for the first few seconds; then as the ablation material approached a full blowing rate, the motion began to diverge and continued to diverge steadily to the end of the run. Figure 2 also shows that injecting nitrogen gas through a porous nose has only a small effect on C_{m_q}. This gas was not phased with the oscillatory motion of the model and therefore does not simulate ablative phase lag experienced by windward-leeward oscillating ablative surfaces. The same pronounced effects obtained by ablation on the cone configurations are also seen on the slender cone-cylinder-flare shapes. Bluntness effects are similar also. Once again, coating the surface of the model aft of the center of rotation (i.e., center of gravity) produced dynamic instability.

Summary

In Ref. 2 it is hypothesized that, for certain re-entry shapes, e.g., "theoretically sharp" slender cones, transition may occur first at the base with accompanying increases in heating and (depending on the heat shield material) with an increase in the ablative blowing rate in this region and possible dynamic instability. Sufficient flight-test data of recent date exist to support this thought. Examination of the ablation tests made at FluiDyne indicates the degree of sensitivity of the damping derivative not only to the presence of ablation but also to its location, whether ahead or behind the center of gravity. Coating the entire model, or forward of the center of gravity, produces a dynamically stable configuration with $C_{m_q} + C_{m_{\dot\alpha}}$ values approaching those for flight test. Coating the rearward sections of a conic or cone-cylinder-flare produces a dynamically unstable vehicle.

If we combine the observed test results and available flight-test data with the transition hypothesis of Sacks and Schurmann,[2] then some of the aerodynamic phenomena associated with advanced re-entry bodies can be explained. As they point out by way of illustration, normal angle-of-attack convergence patterns can be expected during the high-altitude, laminar portion of the trajectory. This would correspond to ablation from the nose or forward sections of the wind-tunnel models, i.e., stabilized C_{m_q}, or convergence. As the vehicle descends further and approaches the transition Reynolds number regime, the angle-of-attack oscillatory pattern may blow up or converge at even a faster rate. Should the flow experience transition at the base first, higher heating rates will be experienced in this area than on the forward sections, and hence marked increase in ablation can be expected. In the tunnel tests, the ablative models coated on the aft sections diverged, i.e., C_{m_q} became positive. Should the flow undergo transition instantaneously, then dynamic instability will not occur and convergence rate will increase. This would correspond to the tunnel test with the ablative models completely coated.

The profound effect of ablation on aerodynamic damping shown in these tests demonstrates that an important physical phenomenon is acting which must be investigated further. Preliminary work has been started to formulate analytical expressions associated with boundary-layer effects on the pressure distributions over an ablating, oscillating body in hypersonic flow. It is also apparent from the analyses that, in order to obtain significant effects on dynamic stability, an aerothermo lag parameter may exist, and the magnitude and sign of this effect on C_{m_q} is dependent upon the center of gravity location. Should subsequent investigations prove the existence of an aerodynamic lag time due to ablation, then a significant parameter has been uncovered to explain behavior of slender re-entry vehicles.

References

[1] Syvertson, C. A. and McDevitt, J. B., "Effects of mass addition on the stability of slender cones at hypersonic speeds," AIAA J. **2**, 939–940 (1963).

[2] Sacks, I. and Schurmann, E. E., "Aerodynamic phenomena associated with advanced reentry systems," Avco-RAD-TM-63-79, pp. 18–22 (October 31, 1963).

Simplified Equations for Determining Propulsion System Specific Impulse

Mario W. Cardullo*
Bellcomm, Inc., Washington, D. C.

Nomenclature

C = const, in.^{2}/lbm
F = thrust, lbf
I_{sp} = theoretical propellant specific impulse, lbf-sec/lbm
I_{ss} = propulsion system specific impulse, lbf-sec/lbm
I_{ssi} = subsystem "i" specific impulse, lbf-sec/lbm
I_t = total impulse, lbf-sec
K = factor less than or equal to unity to account for acceleration, flanges, and welds
M_g = gross stage mass, slugs
M_p = payload mass, slugs
n = number of modules
O/F = oxidizer to fuel weight ratio
P_c = combustion chamber pressure, psia
P = pressure, psia
R = gas constant of pressurant, in./°R
S = design stress, lbf/in.^{2}
t = thickness, in.
t_B = burning time, sec
t_m = minimum wall thickness, in.
T = temperature, °R
v = velocity, fps
V = volume, in.^{3}
α = weight ratio of expelled to total propellant originally in tanks (expulsion efficiency)
β = weight ratio of propellant trapped and/or lost by vaporization to total propellant originally in tanks
γ = ratio of specific heats
ϵ = expansion ratio
η = propellant performance efficiency
ξ = density factor defined in Table 1, lb/in.^{3}
ρ = density, lb/in.^{3}

Subscripts

B = bladder
F = fuel
G = pressurant
O = oxidizer
P = propellant
T = tank

VARIOUS techniques have been used in the past to compare and select propulsion systems. Williams[1] employed the ratio of total impulse to weight to compare various attitude control propulsion systems. A comparison based upon

Received April 1, 1964; revision received September 29, 1964.
* Member of Technical Staff. Member AIAA.